coatings

MDPI

Supplementary Materials:

Influence of Substrate Materials on Nucleation and Properties of Iridium Thin Films Grown by ALD

Paul Schmitt [1,2], Vivek Beladiya [1,2], Nadja Felde [2], Pallabi Paul [1], Felix Otto [3], Torsten Fritz [3], Andreas Tünnermann [1,2] and Adriana V. Szeghalmi [1,2,*]

[1] Institute of Applied Physics IAP, Friedrich Schiller University Jena, Albert-Einstein-Str. 15, D-07745 Jena, Germany; paul.schmitt@iof.fraunhofer.de (P.S.); vivek.beladiya@uni-jena.de (V.B.); pallabi.paul@uni-jena.de (P.P.); andreas.tuennermann@iof.fraunhofer.de (A.T.)

[2] Fraunhofer Institute for Applied Optics and Precision Engineering IOF, Center of Excellence in Photonics, Albert-Einstein-Str. 7, D-07745 Jena, Germany; nadja.felde@iof.fraunhofer.de

[3] Institute of Solid State Physics IFK, Friedrich Schiller University Jena, Helmholtzweg 5, D-07743 Jena, Germany; felix.otto@uni-jena.de (F.O.); torsten.fritz@uni-jena.de (T.F.)

* Correspondence: adriana.szeghalmi@iof.fraunhofer.de; Tel.: +49-3641-807-320

Supplementary Information

As substrate materials, silicon (Si) wafers with a native SiO_2 layer, borosilicate crown glass (BK7), and fused silica (FS), as well as seed layers of SiO_2, TiO_2, Ta_2O_5, Al_2O_3, HfO_2, Ru, Cr, Mo, and graphite (C) deposited on FS substrates, were used. The metal oxide seed layers were grown by atomic layer deposition (ALD), with their process parameters summarized in Table S1. Further information about the deposition tools, precursor materials, and layer properties of SiO_2 and Ta_2O_5 [1], TiO_2 [2], Al_2O_3 and HfO_2 [3] can be found in the references. The metallic and C seed layers were grown by physical vapor deposition (PVD) using direct current (DC) magnetron sputtering with argon (Ar) as sputtering gas. Their process parameters are summarized in Table S2 with further information about Ru and Mo [4] and Cr [5] in the references.

Citation: Schmitt, P.; Beladiya, V.; Felde, N.; Paul, P.; Otto, F.; Fritz, T.; Tünnermann, A.; Szeghalmi, A.V. Influence of Substrate Materials on Nucleation and Properties of Iridium Thin Films Grown by ALD. *Coatings* 2021, *10*, x. https://doi.org/10.3390/xxxxx

Received: 18 December 2020
Accepted: 29 January 2021
Published: 2 February 2021

Publisher's Note: MDPI stays neutral with regard to jurisdictional claims in published maps and institutional affiliations.

Copyright: © 2021 by the authors. Submitted for possible open access publication under the terms and conditions of the Creative Commons Attribution (CC BY) license (http://creativecommons.org/licenses/by/4.0/).

Table S1. Process parameters for the metal oxide seed layers grown by atomic layer deposition (ALD). The precursors tris(dimethylamino)silane (3DMAS), titanium(IV) isopropoxide (TTIP), tantalum(V) ethoxide (TAETO), trimethylaluminum (TMA), and tetrakis(dimethylamino)hafnium(IV) (TDMAH), as well as oxygen plasma (O_2*) or water (H_2O) as co-reactants, were applied.

Substrate Material	Precursor/ Co-reactant	Substrate Temperature T (°C)	ALD Cycle Times [1] t (s)	Plasma Power P (W)
SiO_2 ALD	3DMAS/O_2*	100	0.4 + 4 (hold)/5/3/3	300
TiO_2 ALD	TTIP/O_2*	100	1.5/7/6/4	300
Ta_2O_5 ALD	TAETO/H_2O	250	1.6/6/2/10	–
Al_2O_3 ALD	TMA/O_2*	100	0.03/5/5/2.5	300
HfO_2 ALD	TDMAH/O_2*	100	0.5 + 4 (hold)/10/10/15	300

[1] ALD cycles times consist of precursor pulse/precursor purge/co-reactant pulse/co-reactant purge.

Table S2. Process parameter for the seed layers grown by physical vapor deposition (PVD). These seed layers were deposited by direct current (DC) magnetron sputtering with argon (Ar) as sputtering gas.

Substrate Material	Sputter Target	Base Pressure p (Pa)	Cathode Power P (W)	Ar Flow Rate q (sccm)
Ru PVD	ruthenium	8.9×10^{-5}	500	8
Cr PVD	chromium	2.5×10^{-5}	800	8
Mo PVD	molybdenum	8.0×10^{-5}	580	6
C PVD	carbon	8.0×10^{-5}	1000	6

Table S3 summarizes the properties of the substrate materials, namely the layer thickness, surface roughness, layer density, and morphology, before the iridium (Ir) deposition. For the bare substrates of Si wafers, BK7, and FS, their thickness and density (in brackets) are given according to the specifications of the manufacturer.

Table S3. Properties of the bare substrates and seed layers before the iridium (Ir) deposition. The thickness, density, and surface roughness were determined by X-ray reflectivity (XRR) and atomic force microscopy (AFM).

Substrate Material	XRR Layer Thickness d (nm)	AFM Surface Roughness σ (nm rms)	XRR Layer Density ϱ (g/cm³)	Morphology/ Structure
Si wafer	(675 µm)	0.15 ± 0.02	(2.33)	single-crystalline
BK7	(1.0 mm)	1.93 ± 0.19	(2.51)	amorphous
Fused silica	(1.0 mm)	0.26 ± 0.03	(2.26)	amorphous
SiO_2 ALD	23.8 ± 1.0	0.52 ± 0.05	2.11 ± 0.20	amorphous
TiO_2 ALD	23.1 ± 1.0	0.48 ± 0.05	3.75 ± 0.20	amorphous
Ta_2O_5 ALD	20.3 ± 1.0	0.49 ± 0.05	7.82 ± 0.20	amorphous
Al_2O_3 ALD	25.4 ± 1.0	0.46 ± 0.05	2.90 ± 0.20	amorphous
HfO_2 ALD	21.2 ± 1.0	0.46 ± 0.05	7.70 ± 0.20	amorphous
Ru PVD	18.8 ± 1.0	0.30 ± 0.03	12.20 ± 0.20	poly-crystalline
Cr PVD	20.2 ± 1.0	0.47 ± 0.05	7.24 ± 0.20	poly-crystalline
Mo PVD	21.8 ± 1.0	0.94 ± 0.09	10.10 ± 0.20	poly-crystalline
C PVD	31.2 ± 1.0	0.43 ± 0.04	2.09 ± 0.20	amorphous

The surface free energy of bare substrates and seed layers was determined by wetting analysis. For the wetting analysis, the (most stable) equilibrium contact angle was determined by dynamic measurements using deionized water (H_2O) as measuring liquid under ambient conditions. The surface free energy was calculated using the equation of state by Neumann [6]. In order to evaluate changes in surface free energy due to the Ir deposition, the substrate materials were also characterized after a pre-treatment. This pre-treatment imitates the deposition conditions and equals the Ir ALD deposition procedure with 30 cycles but without an actual Ir deposition. In Table S4, the equilibrium contact angle and

calculated surface free energy of the untreated and pre-treated substrate materials before the Ir deposition are summarized.

Table S4. Equilibrium contact angle and calculated surface free energy of untreated and pre-treated substrate materials before the Ir deposition. The pre-treatment imitates the Ir deposition conditions and equals the Ir ALD deposition procedure with 30 cycles but without an actual Ir deposition. For the surface free energy calculation, the solid-liquid tension was determined using the equation of state by Neumann [6].

Substrate Material	Equilibrium Contact Angle		Surface Free Energy	
	@ Untreated θ (°)	@ Pre-Treated θ (°)	@ Untreated γ (mJ/m²)	@ Pre-Treated γ (mJ/m²)
Si wafer	51.0 ± 2.3	30.2 ± 4.4	53.1 ± 1.7	64.3 ± 2.5
BK7	51.6 ± 1.5	39.0 ± 7.0	52.8 ± 1.1	59.9 ± 4.6
Fused silica	–	27.3 ± 0.6	–	65.7 ± 0.3
SiO_2 ALD	56.7 ± 1.9	30.8 ± 1.5	49.8 ± 1.4	64.1 ± 0.8
TiO_2 ALD	60.1 ± 10.3	69.9 ± 0.5	47.7 ± 7.4	41.7 ± 0.4
Ta_2O_5 ALD	59.6 ± 5.3	65.1 ± 5.0	48.0 ± 3.9	44.7 ± 3.5
Al_2O_3 ALD	95.8 ± 1.0	71.5 ± 1.0	25.6 ± 0.4	43.2 ± 0.7
HfO_2 ALD	83.8 ± 6.5	68.1 ± 5.8	33.1 ± 3.7	42.9 ± 4.0
Ru PVD	69.7 ± 3.7	48.4 ± 1.7	41.9 ± 2.6	54.6 ± 1.2
Cr PVD	93.5 ± 0.8	68.6 ± 0.8	27.0 ± 0.4	42.5 ± 0.5
Mo PVD	68.6 ± 3.0	46.3 ± 2.6	72.1 ± 3.5	55.8 ± 1.8
C PVD	61.6 ± 11.4	62.4 ± 10.8	46.8 ± 8.2	46.3 ± 7.8

The Ir nucleation delay (ND) of the linear thickness growth regime correlates with the surface free energy of the corresponding untreated substrate materials, as Figure S1 illustrates. As with pre-treated substrates, the higher the surface free energy of the untreated substrate materials, the smaller the ND of the Ir coatings and vice versa (see also Figure 8b in the article). Again, this relationship between the Ir ND of the thickness growth regime and surface free energy of the untreated substrates is not strictly linear, but the correlation is clearly visible. Although the pre-treatment of the bare substrates and seed layers changes their surface free energy, the correlation with the ND remains. For most substrate materials, the pre-treatment causes an increase in their surface free energy. For the C seed layer, the value stays constant, and for the TiO_2, Ta_2O_5, and Mo seed layers, the surface free energy decreases (also compare Supplementary Table S4). However, the Mo seed layer is a special case because its surface dewets due to the high substrate temperature of 380 °C.

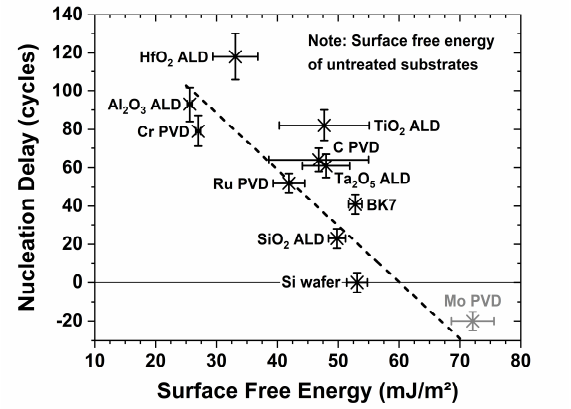


Figure S1. Iridium nucleation delay (ND) of thickness growth regime correlates with the surface free energy of the corresponding (untreated) substrate materials. The lower the wettability of the substrate, the higher the ND for the Ir ALD coating. This correlation persists for both the pre-treated and untreated substrate materials.

Figure S2 shows the X-ray diffraction (XRD) pattern of iridium coatings (with 800 cycles corresponding to 50–60 nm layer thickness) by atomic layer deposition on different substrate materials. For clarity, the diffractograms are vertically shifted. The diffraction peaks are indicated according to Laue. As a reference, the diffraction peaks of a randomly oriented iridium powder sample are shown as red bars [7]. On the Si wafer, the Ir(220) peak is superimposed by the significantly stronger Si(400) peak at nearly the same diffraction angle. The broad peak for BK7 and FS (and seed layers deposited on FS) from about 14°–35° and 14°–30°, respectively, originate from their short-range crystalline order. At a diffraction angle of about 25.4°, a small TiO_2(101) anatase peak is visible. For the Ru seed layer, the Ru(100), Ru(002), and Ru(101) peak at diffraction angles of 38.4°, 42.2°, and 44.0°, respectively, are present. For the Cr seed layer, the Cr(110) peak at a diffraction angle of 44.5° is weakly pronounced. The Mo(110) peak at a diffraction angle of 40.5° is superimposed by the significantly stronger Ir(111) peak on the Mo seed layer.

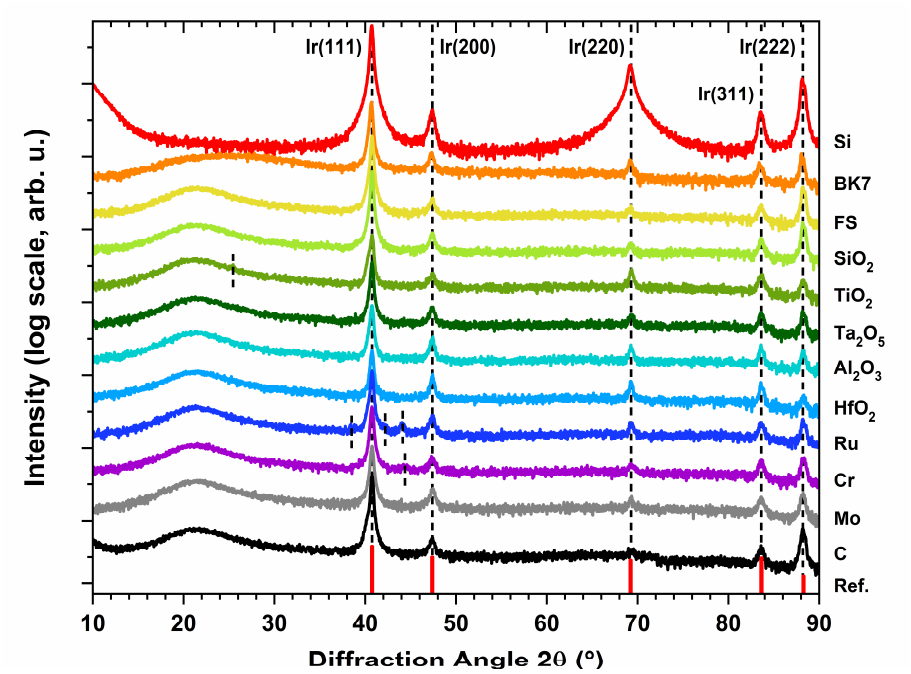


Figure S2. X-ray diffraction (XRD) pattern of Ir coatings (with 800 cycles corresponding to 50–60 nm layer thickness) on different substrate materials. For clarity, the diffractograms are vertically shifted. The diffraction peaks are indicated according to Laue. As a reference , the diffraction peaks of an Ir powder sample are shown as red bars [7].

The iridium ALD coatings show a preferred orientation of the crystallographic Ir(111) plane on all substrate materials. For a randomly oriented iridium powder sample, the two most intense diffraction peaks, Ir(111) and Ir(200), have a ratio of I(111)/I(200) = 2 [7]. Here, the ratio I(111)/I(200) of the iridium coatings varies between about 6 on the HfO_2 seed layer and about 122 on the Si wafer. Consequently, the crystallographic Ir(111) plane is preferred, also compared to all other orientations in the iridium layers. The calculated XRD peak ratios of the iridium coatings on different substate materials and the powder reference sample are summarized in Table S5.

Table S5. X-ray diffraction peak ratios of Ir coatings on different substrate materials and a powder reference sample [7].

Substrate Material	X-ray Diffraction Peak Ratios (arb. u.)			
	I(111)/I(200)	I(111)/I(220)	I(111)/I(311)	I(111)/I(222)
Si wafer	122.2	-	165.9	523
BK7	36.2	63.6	70.2	253
Fused silica	82.0	184.6	130.0	462
SiO_2 ALD	77.3	211.3	99.3	472
TiO_2 ALD	18.9	12.6	17.4	84
Ta_2O_5 ALD	25.2	64.3	34.3	149
Al_2O_3 ALD	10.1	19.8	16.0	99
HfO_2 ALD	6.2	10.5	11.0	58
Ru PVD	22.9	43.5	37.2	156
Cr PVD	35.1	96.5	43.6	159
Mo PVD	22.7	51.8	42.8	136
C PVD	74.3	257.9	130.6	415
Ref. [7]	2.0	2.4	2.1	7

References

1. Pfeiffer, K.; Schulz, U.; Tünnermann, A.; Szeghalmi, A. Antireflection coatings for strongly curved glass lenses by atomic layer deposition. *Coatings* **2017**, *7*, 118, doi:10.3390/coatings7080118.
2. Ratzsch, S.; Kley, E.-B.; Tünnermann, A.; Szeghalmi, A. Influence of the oxygen plasma parameters on the atomic layer deposition of titanium dioxide. *Nanotechnology* **2015**, *26*, 24003, doi:10.1088/0957-4484/26/2/024003.
3. Shestaeva, S.; Bingel, A.; Munzert, P.; Ghazaryan, L.; Patzig, C.; Tünnermann, A.; Szeghalmi, A. Mechanical, structural, and optical properties of PEALD metallic oxides for optical applications. *Appl. Opt.* **2017**, *56*, C47–C59, doi:10.1364/AO.56.000C47.
4. Müller, R.; Yulin, S.; Naujok, P.; Kaiser, N.; Tünnermann, A. Optical properties and oxidation resistance of different transition metals for soft X-ray and EUV applications. *Thin Solid Film.* **2017**, *624*, 1–6, doi:10.1016/j.tsf.2017.01.016.
5. Yulin, S.A.; Kuhlmann, T.; Feigl, T.; Kaiser, N. Reflectivity and stability of Cr/Sc multilayers for the soft X-ray range. *Proc. SPIE* **2002**, *4782*, 285–291, doi:10.1117/12.451350.
6. Li, D.; Neumann, A.W. Equation of state for interfacial tensions of solid-liquid systems. *Adv. Colloid Interface Sci.* **1992**, *39*, 299–345, doi:10.1016/0001-8686(92)80064-5.
7. Swanson, H.E.; Tatge, E. *Standard X-ray Diffraction Powder Patterns*; National Bureau of Standards: Washington, D.C., USA, 1955.